



Photocatalytic degradation of gaseous 1-propanol using an annular reactor: Kinetic modelling and pathways

G. Vincent, P.M. Marquaire, O. Zahraa*

Département de Chimie Physique des Réactions, UMR 7630 CNRS, Nancy-Université, ENSIC, 1 rue Grandville, BP 20451, 54001 Nancy Cedex, France

ARTICLE INFO

Article history:

Received 22 November 2007
Received in revised form 5 March 2008
Accepted 18 April 2008
Available online 24 April 2008

Keywords:

Reactor modelling
Alcohols
Photocatalytic degradation mechanism
Two-site kinetic model
Aldehydes

ABSTRACT

Photocatalytic oxidation of airborne contaminants appears to be a promising process for remediation of air polluted by Volatile Organic Compounds (VOCs). In the present work, the photocatalytic oxidation of gaseous 1-propanol has been investigated by using an annular photoreactor. The annular photocatalytic reactor was modelled by a cascade of heightened elementary continuously stirred tank reactors. The influence of several kinetic parameters such as pollutant concentration, incident light irradiance, contact time and humidity content has been studied. The photocatalytic degradation by-products of 1-propanol has been identified in the gas-phase by GC/MS. Propionaldehyde and acetaldehyde were found to be the main gaseous intermediates. Propionaldehyde and acetaldehyde have been taken into account in a “two-site model” to evaluate the possible competition of adsorption between 1-propanol and its by-products of degradation. A mechanistic pathway is then proposed for the photocatalytic degradation of 1-propanol.

© 2008 Elsevier B.V. All rights reserved.

1. Introduction

1-Propanol is widely used as solvent, chemical intermediate, ruminant feed supplement and flavour in foods. Emission of 1-propanol via waste gases and wastewater occurs in industry, and diffuse airborne emissions occur during the use of this compound. Volatile Organic Compounds (VOCs) are well known to be malodorous, toxic and VOC emissions contribute to global warming [1]. Vapour phase 1-propanol can provoke eye, nose and throat irritation. The irritation value seems to be about 400 ppm (1000 mg m⁻³) for an exposition from 3 to 5 min. 1-Propanol has threshold limit value (TLV) in air of 200 ppm (500 mg m⁻³). The TLV is the maximum permissible concentration of a pollutant generally defined in workplace atmospheres. A degradation process could be used to reduce VOC emissions in workplace atmospheres.

Vapour phase 1-propanol is degraded in the atmosphere by reaction with photochemically-produced hydroxyl radicals OH•. Therefore, photocatalytic oxidation appears to be a possible method of elimination [2]. Heterogeneous photocatalysis using mainly titanium dioxide (TiO₂) offers several advantages: (1) the catalyst is inexpensive, (2) it operates at ambient temperature, (3) the mineralization products are mainly CO₂ and H₂O and

(4) no other chemical reagent is needed [3]. The alcohol photocatalytic degradation is well known to produce by-products in gas-phase or at the catalyst surface [4–13]. Recently, several authors have studied the photocatalytic degradation of ethanol in the gas-phase: doped TiO₂ (Fe, Pd and Cu) [5], TiO₂ P25 on glass plate [14], incorporation of TiO₂ P25 onto polymers [10] etc. Nimlos et al. [9] have investigated the photocatalytic degradation of ethanol and have established the following reaction pathway: ethanol → acetaldehyde → acetic acid → formaldehyde → formic acid → carbon dioxide. Chen et al. [15] and Araña et al. [7] have revealed that the corresponding carboxylic acid appears as an intermediate of the selected alcohol degradation. Benoît-Marquié et al. [8] have proposed the following degradation mechanism during the 1-butanol photocatalytic degradation: 1-butanol → butanal → butanoic acid → propionaldehyde and 1-propanol.

This work focuses on the photocatalytic degradation of 1-propanol. The first part of this work consists summarizing the results of the kinetic study carried out on this pollutant. Our annular photocatalytic reactor was modelled by a cascade of continuously stirred tank reactors (CSTR) in order to predict the 1-propanol conversion and the by-product concentrations. A “two-site model” was developed based on studies addressing multi-site binding of alcohols and other oxygenated hydrocarbons. In the second part of this work, a possible mechanistic pathway has been established, compared with results obtained by the authors previously quoted.

* Corresponding author. Tel.: +33 3 83 17 51 18; fax: +33 3 83 37 81 20.
E-mail address: Orfan.Zahraa@ensic.inpl-nancy.fr (O. Zahraa).

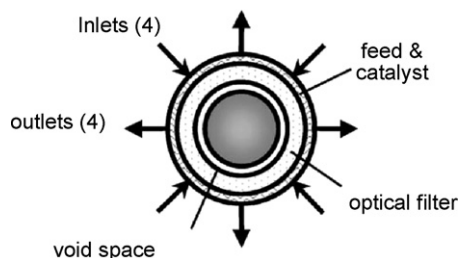


Fig. 1. Schematic representation of annular photocatalytic reactor.

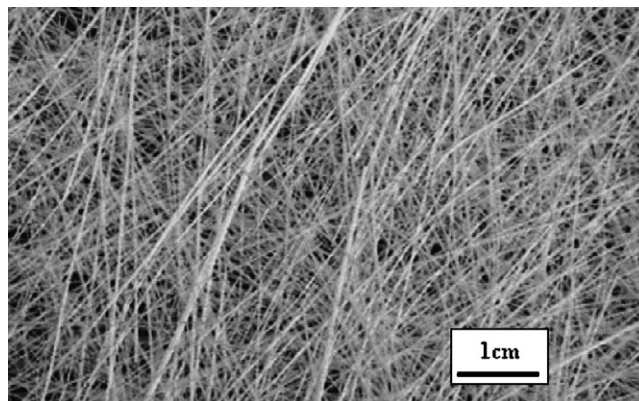


Fig. 2. Optical picture of fibreglass support.

2. Experimental

2.1. Experimental set-up and procedure

The annular photocatalytic reactor was equipped with four inlets and four outlets in order to ensure a good flow distribution (Fig. 1). A fibreglass support (effective porosity $\varepsilon = 0.95$) impregnated with TiO_2 Degussa P25 was inserted between two Pyrex glass tubes with a thickness of 1.8 mm. This low thickness provides a best contact between polluted air and photocatalyst. A commercially Philips® TLD 18W/08 fluorescent tube is placed in the centre of the unit offering the best conditions of light irradiance. It can be noticed that the UV lamp has a spectral peak centred at about 365 nm. The fluorescent tube and the photocatalyst were separated by a liquid filter in order to control both temperature and light irradiance during the degradation process. The light transmission was attenuated by a specific nigrosine concentration in aqueous solution. The total diameter, the volume and the photoactive length of the annular reactor were, respectively, 5.2 cm, 66.4 cm^3 and 25 cm. The diameter of the space for the fluorescent tube was 30.5 mm. The fibreglass support apparent area exposed to UV was 360 cm^2 . The experimental unit permits to generate a polluted air with a specific VOC concentration and humidity content. The functioning of the experimental set-up has been widely detailed in previous works [16,17]. Several kinetic parameters can be tested on the photocatalytic degradation efficiency as initial concentration of pollutant, light irradiance, contact time and humidity content.

The GC is a Hewlett Packard 5890 Series II apparatus equipped with a FID. The GC operational parameters were as follows: analytical column, Porapak Q column 1/8" (1 m) at 180°C ; carrier gas, nitrogen and hydrogen at 20 and 10 mL min^{-1} ; injected volume, 1 cm^3 ; FID detector at 250°C supplied with air/hydrogen at 300 and 60 mL min^{-1} , respectively.

The by-products generated during the photocatalytic degradation of 1-propanol were identified by GC/MS. The intermediates have been simply sampled with a gaseous syringe through a septum at the photoreactor exit and directly injected into the GC/MS apparatus. The GC/MS is an Agilent 6850 Series apparatus equipped with a mass selective detector (MSD) Agilent 5973 Network. The GC/MS operational parameters were as follows: analytical column, HP Plot Q ($30 \text{ m} \times 0.32 \text{ mm i.d.}$); carrier gas, helium at 1.5 mL min^{-1} ; program of temperature, 30°C for 10 min, $25^\circ\text{C min}^{-1}$ and 180°C for 20 min; temperature of injector, 250°C (splitless); detector, MSD at 250°C .

2.2. Catalyst preparation

The catalyst consisted in TiO_2 P25 Degussa deposited on a Sintomat® fibreglass support ($250 \text{ mm} \times 144 \text{ mm}$). A single rectangular section of fibreglass support (360 cm^2) was inserted inside the photoreactor. From Fig. 2, the fibreglass support is like a mat of thickness 1.8 mm, where fibre bundles of rectangular section

$300 \mu\text{m} \times 40 \mu\text{m}$ are randomly oriented. The catalyst deposition followed a specific protocol more detailed in a previous work [18]. TiO_2 P25 Degussa was dispersed in an aqueous suspension adjusted at pH 3 with nitric acid in order to prevent the titanium dioxide aggregation. The fibreglass support was impregnated with this suspension. After complete evaporation of water, the support was dried at 100°C for 1 h and fired at 475°C for 4 h to ensure a good adherence between catalyst and support. About 38 mg of TiO_2 was deposited on fibreglass support.

3. Photocatalytic results and discussion

3.1. Annular photoreactor modelling

The residence time distribution (RTD) of a chemical reactor is a description of the time that different fluid elements spend inside the reactor. Experiments of RTD, using a pulse of hydrogen in the feed detected at the photoreactor exit by a thermal conductivity detector (TCD), revealed a cascade of eighteen elementary continuously stirred tank reactors ($J = 18$) as illustrated in Fig. 3. Details about RTD can be obtained in previous works [17,19]. It is generally accepted that above a number of 20 elementary reactors, the experimental reactor can be considered practically as a plug flow reactor (PFR). In the case of continuously stirred tank reactors, the

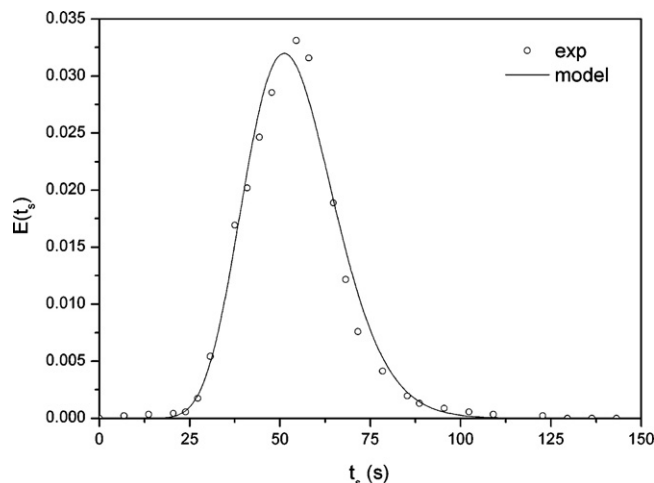


Fig. 3. Residence time distribution $E(t_s)$ of the annular photoreactor ($J = 18$).

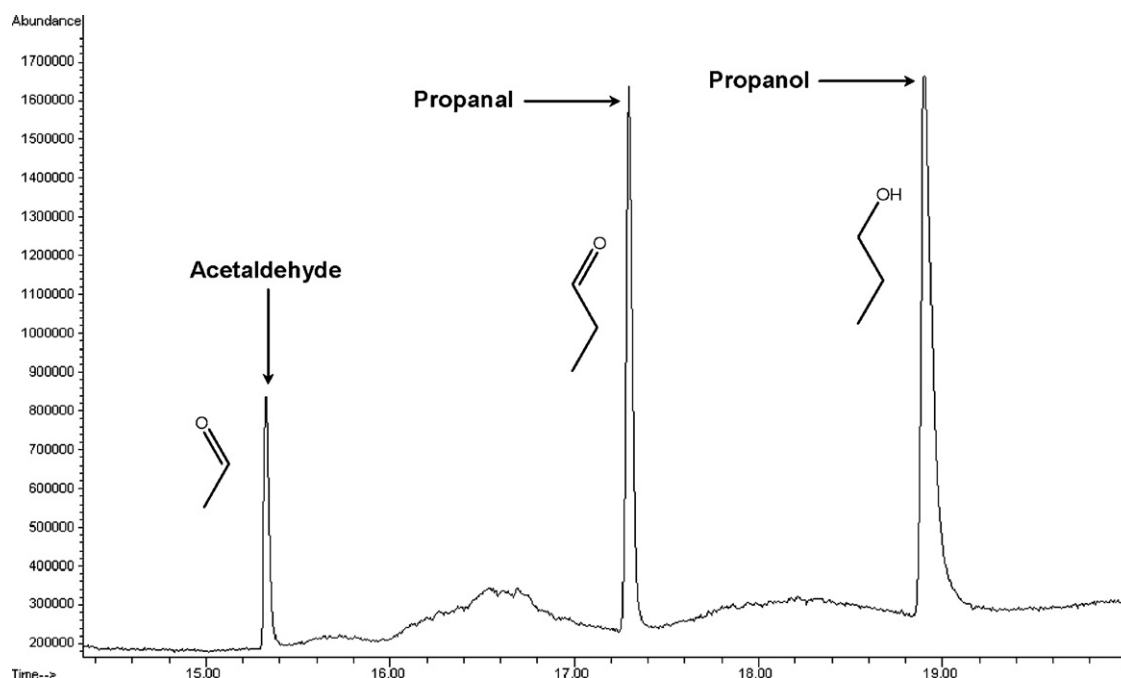


Fig. 4. Typical effluent chromatogram with acetaldehyde, propionaldehyde (propanal) and 1-propanol (propanol) identified by GC/MS.

expression of RTD takes the following form [19]:

$$E(t_s) = \left(\frac{J}{\bar{t}_s}\right)^J \frac{t_s^{J-1} \exp(-Jt_s/\bar{t}_s)}{(J-1)!} \quad (1)$$

where $E(t_s)$ is the residence time distribution, t_s the time, J the total number of continuously stirred tank reactors and \bar{t}_s is the main residence time.

3.2. Conversion and identification of by-products

A gas chromatograph equipped with a flame ionization detector (FID) was used to follow 1-propanol concentration during photocatalytic oxidation. Finally the 1-propanol conversion X in the reactor is expressed by the following equation:

$$X = 1 - \frac{C_{out}}{C_{in}} \quad (2)$$

where C_{in} is the inlet and C_{out} the outlet 1-propanol concentration, respectively. It is worthwhile to notice that all the obtained results were measured after a defined stabilization period from 130 to 200 min.

The gaseous intermediates, produced during the photocatalytic degradation of 1-propanol, were identified by GC/MS and were quantified by GC/FID. Fig. 4 shows a typical chromatogram of the effluent obtained after 1-propanol photocatalytic oxidation. Acetaldehyde, propionaldehyde (propanal) and 1-propanol were detected at 15.3, 17.3 and 18.9 min, respectively. It can be noticed that Araña et al. [4,6] have identified propionaldehyde, propionic acid and acetaldehyde during the 1-propanol photocatalytic degradation.

3.3. Effect of the 1-propanol concentration

The effect of initial pollutant concentration C_0 on the photocatalytic rate was investigated in the range of 100–300 ppm. In photocatalytic studies, kinetics of photodegradation are generally expressed by the Langmuir-Hinshelwood (LH) model. Eq. (3) considers that the adsorption of reaction intermediates and products

is not significant. In this present work, this expression was called “simple LH model” [20]:

$$r = k \frac{KC}{1 + KC} \quad (3)$$

where r is the rate of photodegradation (ppm min^{-1}), k an apparent kinetic constant (ppm min^{-1}), K the adsorption constant (ppm^{-1}) and C is the pollutant concentration (ppm). The evolution of the 1-propanol concentration and conversion through the annular photoreactor, with $J=18$ CSTR, are defined by the set of J mass balance expressions:

$$C_j = C_{j-1} - \varepsilon \frac{V}{JQ_v} \left[\frac{kKC_j}{1 + KC_j} \right] \quad (4)$$

$$X = 1 - \frac{C_j}{C_0} \quad (5)$$

$$\varepsilon = \frac{\text{volume occupied by the flowing fluid}}{\text{total volume of photoreactor}} = \frac{Q_v}{V} \times \bar{t}_s \quad (6)$$

where Q_v is the total volume flow rate, ε the effective porosity, C_j the outlet pollutant concentration of the reactor “ j ”, C_{j-1} the inlet pollutant concentration of the reactor “ j ”, C_j the optimised pollutant concentration at the photoreactor outlet, C_0 the initial concentration and V is the total volume of photoreactor. The constants k and K were adjusted via an optimisation program with a minimised value of χ^2 , which is defined as below:

$$\chi^2 = n_{\text{exp}}^{-1} \sum_{i=1}^{n_{\text{exp}}} (C_{j,i} - C_{j,\text{exp},i})^2 \quad (7)$$

where n_{exp} is the total number of experiments, C_j the optimised pollutant concentration at the photoreactor outlet, $C_{j,\text{exp}}$ the experimental pollutant concentration at the photoreactor outlet and i is the experiment number for a given initial concentration.

This expression (Eq. (3)) does not take into account possible by-products. The following expression has been suggested to account for reactions involving competition between two or more species

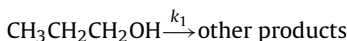
on a single adsorption site:

$$r = k \frac{KC}{1 + KC + \sum_x K_x C_x} \quad (8)$$

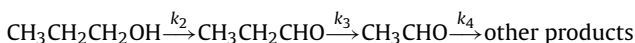
where K_x is the adsorption constant for by-product x and C_x the concentration of by-product x in the gas phase. We only focus on propionaldehyde and acetaldehyde as reaction intermediates.

Nimlos et al. [9] have studied the photocatalytic degradation of ethanol and they have modified the adsorption model to include the possibility of two adsorption sites. Spectroscopic studies have demonstrated that alcohols and organic acids can dissociate upon adsorption to TiO_2 to form RO^- and RO_2^- groups. It has been suggested that this occurs at oxygen bridging sites. It can be noticed that this type of bonding is unlikely with aldehydes. Polar organic compounds can form hydrogen bond to the OH groups on the TiO_2 surface. In this case, the alcohols, acids and aldehydes could all bind to these sites. In this present work, Type I site is assumed suitable for the adsorption of alcohols and acids, while Type II site can accommodate all of the organic compounds considered [21]. In this present work, we have only focused on the by-products quantified in the gas phase. The “two-site model” can be written as below:

Type I:



Type II:



Therefore, the evolution of 1-propanol concentration through the annular photoreactor, with $J=18$ CSTR, can be defined by the set of J mass balance expression with the “two-site model”:

$$C_j = C_{j-1} - \varepsilon \frac{V}{JQ_v} (k_1 \theta_I + k_2 \theta_{II}) \quad \text{with } \theta_I = \frac{K_1 C_j}{1 + K_1 C_j},$$

$$\theta_{II} = \frac{K_2 C_j}{1 + K_2 C_j + K_3 C'_j + K_4 C''_j} \quad (9)$$

$$C_j = C_{j-1} - \varepsilon \frac{V}{JQ_v} \left[\left(\frac{k_1 K_1 C_j}{1 + K_1 C_j} \right) + \left(\frac{k_2 K_2 C_j}{1 + K_2 C_j + K_3 C'_j + K_4 C''_j} \right) \right] \quad (10)$$

where θ_I is the surface coverage of pollutant on the Type I site and θ_{II} the surface coverage of pollutant on the Type II site. Then the evolution of propionaldehyde concentration through the annular photoreactor, with $J=18$ CSTR, is defined by the following expression considering only the Type II site:

$$C'_j = C'_{j-1} + \varepsilon \frac{V}{JQ_v} \left[\frac{k_2 K_2 C_j}{1 + K_2 C_j + K_3 C'_j + K_4 C''_j} \right]$$

$$- \varepsilon \frac{V}{JQ_v} \left[\frac{k_3 K_3 C'_j}{1 + K_2 C_j + K_3 C'_j + K_4 C''_j} \right] \quad (11)$$

And the evolution of acetaldehyde concentration through the annular photoreactor, with $J=18$ CSTR, is defined as below considering only the Type II site:

$$C''_j = C''_{j-1} + \varepsilon \frac{V}{JQ_v} \left[\frac{k_3 K_3 C'_j}{1 + K_2 C_j + K_3 C'_j + K_4 C''_j} \right]$$

$$- \varepsilon \frac{V}{JQ_v} \left[\frac{k_4 K_4 C''_j}{1 + K_2 C_j + K_3 C'_j + K_4 C''_j} \right] \quad (12)$$

Table 1
Kinetic and adsorption constants

	“Simple LH model”	“Two-site model”
1-Propanol	$k = 1024 \text{ ppm min}^{-1}$ $K = 0.014 \text{ ppm}^{-1}$	$k_1 = 141.6 \text{ ppm min}^{-1}$ (Type I) $K_1 = 0.021 \text{ ppm}^{-1}$ $k_2 = 870.2 \text{ ppm min}^{-1}$ (Type II) $K_2 = 6.44 \text{ ppm}^{-1}$
Propionaldehyde		$k_3 = 2701 \text{ ppm min}^{-1}$ (Type II) $K_3 = 4.45 \text{ ppm}^{-1}$
Acetaldehyde		$k_4 = 477 \text{ ppm min}^{-1}$ (Type II) $K_4 = 21.18 \text{ ppm}^{-1}$

Regular conditions used were: total volume flow rate, $Q_v = 320 \text{ mL min}^{-1}$; relative humidity, $\text{RH} = 10\%$; photoreactor temperature, $T_R = 30^\circ \text{C}$; incident light irradiance, $I_0 = 1.076 \text{ mW cm}^{-2}$; oxygen content, air (20 vol% O_2). Effect of the initial concentration on the 1-propanol and its by-product outlet concentrations after a 132 min illumination time.

where Q_v is the total volume flow rate, ε the effective porosity, C_j the outlet 1-propanol concentration of the reactor “ j ”, C_{j-1} the inlet 1-propanol concentration of the reactor “ j ”, C'_j the outlet propionaldehyde concentration of the reactor “ j ”, C'_{j-1} the inlet propionaldehyde concentration of the reactor “ j ”, C''_j the outlet acetaldehyde concentration of the reactor “ j ”, C''_{j-1} the inlet acetaldehyde concentration of the reactor “ j ”, V the total volume of photoreactor, k_1 an apparent kinetic constant for 1-propanol on the Type I site, k_2 an apparent kinetic constant for 1-propanol on the Type II site, k_3 an apparent kinetic constant for propionaldehyde on the Type II site, k_4 an apparent kinetic constant for acetaldehyde on the Type II site, K_1 the adsorption constant for 1-propanol on the Type I site, K_2 the adsorption constant for 1-propanol on the Type II site, K_3 the adsorption constant for propionaldehyde on the Type II site and K_4 is the adsorption constant for acetaldehyde on the Type II site. Constants have been optimised via a minimisation of χ^2 expressed as below:

$$\chi^2 = n_{\text{exp}}^{-1} \left[\sum_{i=1}^n (C_{j,i} - C_{j,\text{exp},i})^2 + \sum_{i=1}^n (C'_{j,i} - C'_{j,\text{exp},i})^2 + \sum_{i=1}^n (C''_{j,i} - C''_{j,\text{exp},i})^2 \right] \quad (13)$$

where n_{exp} is the total number of experiments, C_j the optimised 1-propanol concentration at the photoreactor exit, $C_{j,\text{exp}}$ the experimental 1-propanol concentration at the photoreactor exit, C'_j the optimised propionaldehyde concentration at the photoreactor exit, $C'_{j,\text{exp}}$ the experimental propionaldehyde concentration at the photoreactor exit, C''_j the optimised acetaldehyde concentration at the photoreactor exit, $C''_{j,\text{exp}}$ the experimental acetaldehyde concentration at the photoreactor exit and i is the experiment number.

The constant values optimised via solver program are summarised in Table 1. In this present work, two different LH models were used, a “simple LH model”, the other one corresponding to “two-site model”. The 1-propanol conversion is also partially limited by the adsorption of intermediates on the catalyst surface and the profile of 1-propanol does not strictly follow the rate form in Eq. (3). The adsorbed intermediates can block the reactive sites at the catalyst surface and can inhibit the photocatalytic degradation of 1-propanol. Here, we found that a “simple LH model” was inadequate for fitting this 1-propanol conversion curve in Fig. 5 and that best fit could be obtained if intermediates were included. It can be noticed that the 1-propanol conversion decreases slightly with an increase of illumination time. This trend could be attributed to a possible reversible deactivation of photocatalyst, which is well

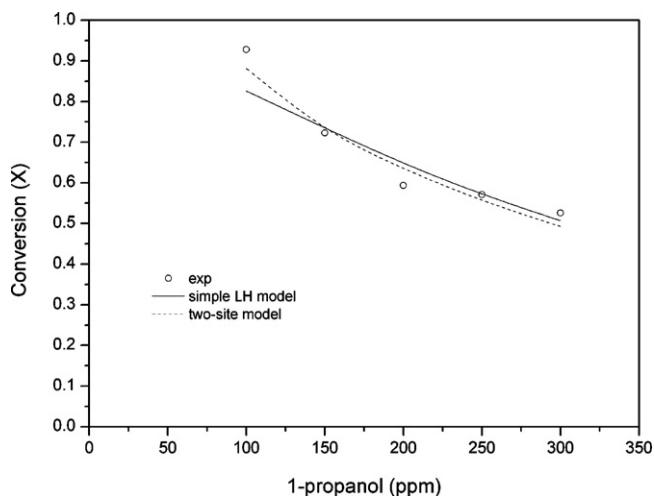


Fig. 5. Effect of the initial concentration on the 1-propanol conversion after a 132 min illumination time. Regular conditions used were: total volume flow rate, $Q_v = 320 \text{ mL min}^{-1}$; relative humidity, $\text{RH} = 10\%$; photoreactor temperature, $T_R = 30^\circ\text{C}$; incident light irradiance, $I_0 = 1.076 \text{ mW cm}^{-2}$; oxygen content, air (20 vol% O_2).

known in this type of reaction or a photostationary state establishment. For these reasons, the photocatalyst was regenerated after each experiment in order to recover its initial activity. From Table 1, it can be noticed that k_2 and k_3 are higher than k_4 , which suggests that the acetaldehyde degradation is slower than propionaldehyde and 1-propanol. From Table 1, it can be also noticed that K_4 is higher than K_2 and K_3 suggesting that the aldehyde adsorption is more important than 1-propanol and propionaldehyde on the Type II site. The constant values optimised can explain the possible accumulation of acetaldehyde at the TiO_2 surface during the 1-propanol photocatalytic degradation. As by-products could be potentially more toxic for the human health than the initial pollutant, identify and quantify them is necessary. The TLV is the maximum permissible concentration of a material, generally expressed in ppm in air for some defined period of time (often 8 h, but sometimes for 40 h per week over an assumed working lifetime). 1-Propanol, propionaldehyde and acetaldehyde have a TLV in air of 200 ppm (500 mg m^{-3}), 20 ppm (48 mg m^{-3}) and 100 ppm (180 mg m^{-3}), respectively. Fig. 6 deals with the predicted outlet concentrations of 1-propanol, propionaldehyde and acetaldehyde. It can be noticed that the outlet concentrations seem to be well fitted with the constants optimised via the “two-site model”. For a 300 ppm inlet concentration of 1-propanol, the value obtained for the exit concentration (C_{out}) of propionaldehyde is higher than its TLV (1-propanol: $C_{\text{out}}/\text{TLV} = 0.7$; propionaldehyde: $C_{\text{out}}/\text{TLV} = 3.1$; acetaldehyde: $C_{\text{out}}/\text{TLV} = 0.4$). This photoreactor seems to be inefficient in our experimental conditions for the photocatalytic degradation of 1-propanol, as it produces intermediates more toxic than the initial pollutant. The inefficiency of the photocatalytic reactor could be explained by the accumulation of aldehydes at the TiO_2 surface. Thus the efficiency could be improved with other experimental conditions such as a higher contact time.

3.4. Effect of the incident light irradiance

The effect of the incident light irradiance on the 1-propanol conversion was investigated in the range of $0.078\text{--}3.94 \text{ mW cm}^{-2}$. The incident light irradiance was measured by an UV-sensible radiometer (VLX-365) and the 3 W light power has been verified by actinometry in a previous work [16]. The light transmission was

attenuated by a nigrosine solution in the temperature-regulated bath. From Wang et al. [22], the kinetic constant is a function of light irradiance as below:

1-Propanol (Type I):

$$k_1 = \beta_1 \times I_0^{\alpha_1} \quad (14)$$

1-Propanol (Type II):

$$k_2 = \beta_2 \times I_0^{\alpha_2} \quad (15)$$

Propionaldehyde (Type II):

$$k_3 = \beta_3 \times I_0^{\alpha_3} \quad (16)$$

Acetaldehyde (Type II):

$$k_4 = \beta_4 \times I_0^{\alpha_4} \quad (17)$$

where β_1 , β_2 , β_3 or β_4 are rate constants independent of incident light irradiance, I_0 the incident light irradiance and α_1 , α_2 , α_3 , α_4 are kinetic orders with respect to I_0 .

Consequently, the evolution of 1-propanol concentration through the annular photoreactor, suggesting the adsorption on two-sites and the possible competition with aldehydes, with $J = 18$ CSTR, is defined by the set of J mass balance expression with the “two-site model”:

$$C_j = C_{j-1} - \varepsilon \frac{V}{JQ_v} \left[\left(\frac{\beta_1 \times I_0^{\alpha_1} \times K_1 C_j}{1 + K_1 C_j} \right) + \left(\frac{\beta_2 \times I_0^{\alpha_2} \times K_2 C_j}{1 + K_2 C_j + K_3 C'_j + K_4 C''_j} \right) \right] \quad (18)$$

Then the evolution of propionaldehyde concentration through the annular photoreactor, with $J = 18$ CSTR, is defined by the following expression:

$$C'_j = C'_{j-1} + \varepsilon \frac{V}{JQ_v} \left[\frac{\beta_2 \times I_0^{\alpha_2} \times K_2 C_j}{1 + K_2 C_j + K_3 C'_j + K_4 C''_j} \right] - \varepsilon \frac{V}{JQ_v} \left[\frac{\beta_3 \times I_0^{\alpha_3} \times K_3 C'_j}{1 + K_2 C_j + K_3 C'_j + K_4 C''_j} \right] \quad (19)$$

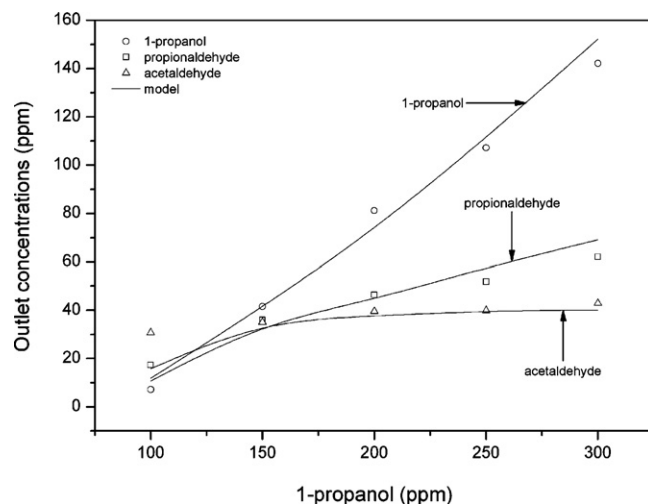


Fig. 6. Effect of the initial concentration on the 1-propanol and its by-product outlet concentrations after a 132 min illumination time. Regular conditions used were: total volume flow rate, $Q_v = 320 \text{ mL min}^{-1}$; relative humidity, $\text{RH} = 10\%$; photoreactor temperature, $T_R = 30^\circ\text{C}$; incident light irradiance, $I_0 = 1.076 \text{ mW cm}^{-2}$; oxygen content, air (20 vol% O_2).

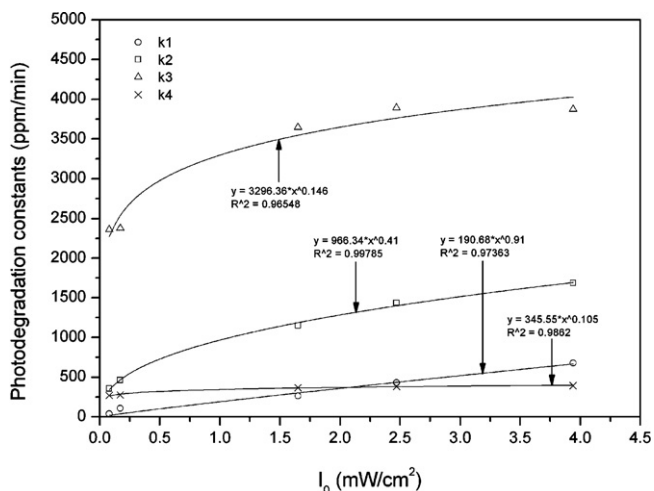


Fig. 7. Effect of the incident light irradiance on the photodegradation constants after a 154 min illumination time. Regular conditions used were: total volume flow rate, $Q_v = 320 \text{ mL min}^{-1}$; relative humidity, $\text{RH} = 10\%$; photoreactor temperature, $T_R = 30^\circ\text{C}$; initial concentration, 1-propanol = 400 ppm; oxygen content, air (20 vol% O_2).

And the evolution of acetaldehyde concentration through the annular photoreactor, with $J = 18$ CSTR, is defined as below:

$$C_j'' = C_{j-1}'' + \varepsilon \frac{V}{JQ_v} \left[\frac{\beta_3 \times I_0^{\alpha_3} \times K_3 C_j''}{1 + K_2 C_j + K_3 C_j'' + K_4 C_j''} \right] - \varepsilon \frac{V}{JQ_v} \left[\frac{\beta_4 \times I_0^{\alpha_4} \times K_4 C_j''}{1 + K_2 C_j + K_3 C_j'' + K_4 C_j''} \right] \quad (20)$$

A plot of k versus I_0 should be proportional to I_0^α and will allow the two constants β and α to be determined (Fig. 7). The kinetic orders are summarised in Table 2. It can be noticed that k_1 , k_2 , k_3 and k_4 are proportional to $I_0^{0.91}$ (1-propanol Type I), $I_0^{0.41}$ (1-propanol Type II), $I_0^{0.15}$ (propionaldehyde Type II) and $I_0^{0.11}$ (acetaldehyde Type II), respectively. From Fig. 8, 1-propanol conversion rate increases dramatically from 0.17 to 0.75 as the light irradiance enhances from 0.078 to 3.94 mW cm^{-2} . We found that a “two-site model” was adequate for fitting the 1-propanol conversion curve in Fig. 8. The kinetic order values were lower than 1, suggesting that the rate of electron-hole formation exceeds the rate of photocatalytic oxidation, resulting in electron-hole recombination. It can be noticed that at low light irradiance, r is a linear function to I_0 (first-order kinetic) [23]. At medium light irradiance, r is a

Table 2
Kinetic orders and adsorption constants

	“Two-site model”
1-Propanol	$\alpha_1 = 0.91$ (Type I) $K_1 = 0.021 \text{ ppm}^{-1}$ $\alpha_2 = 0.41$ (Type II) $K_2 = 6.44 \text{ ppm}^{-1}$
Propionaldehyde	$\alpha_3 = 0.15$ (Type II) $K_3 = 4.45 \text{ ppm}^{-1}$
Acetaldehyde	$\alpha_4 = 0.11$ (Type II) $K_4 = 21.18 \text{ ppm}^{-1}$

Effect of the incident light irradiance on the 1-propanol and its by-product outlet concentrations after a 154 min illumination time. Regular conditions used were: total volume flow rate, $Q_v = 320 \text{ mL min}^{-1}$; relative humidity, $\text{RH} = 10\%$; photoreactor temperature, $T_R = 30^\circ\text{C}$; initial concentration, 1-propanol = 400 ppm; oxygen content, air (20 vol% O_2).

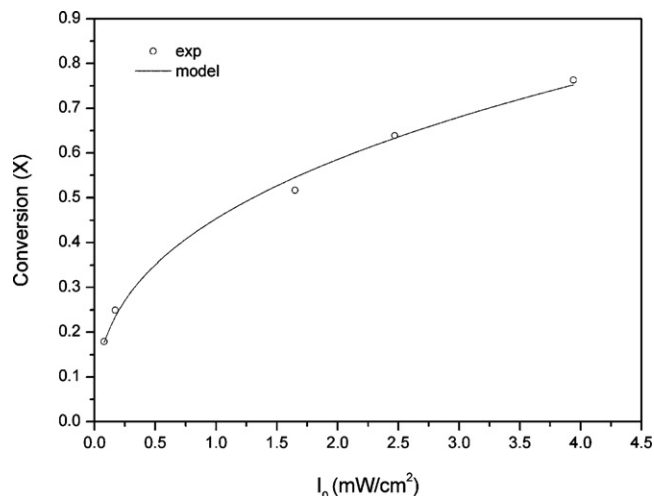


Fig. 8. Effect of the incident light irradiance on the 1-propanol conversion after a 154 min illumination time. Regular conditions used were: total volume flow rate, $Q_v = 320 \text{ mL min}^{-1}$; Relative humidity, $\text{RH} = 10\%$; photoreactor temperature, $T_R = 30^\circ\text{C}$; initial concentration, 1-propanol = 400 ppm; oxygen content, air (20 vol% O_2).

linear function of $I_0^{0.5}$ (half-order kinetic) [23]. From Fig. 9, it can be noticed that the outlet 1-propanol concentration decreases dramatically whereas propionaldehyde and acetaldehyde concentrations increase slightly as the light irradiance enhances from 0.078 to 3.94 mW cm^{-2} . About 1-propanol, kinetic orders are specific to site nature (Type I, $\alpha = 0.91$ and Type II, $\alpha = 0.41$). In a previous study, Vincent et al. [24] have found that hydroxyl radical recombination can occur in photocatalysis when $\alpha < 0.5$ without mass transfer limitations. The incident light irradiance seems to have a low effect on the by-product concentrations. By-products are generated on Type II sites via the following pathway: 1-propanol \rightarrow propionaldehyde \rightarrow acetaldehyde \rightarrow other by-products. Their concentrations do not vary much compared to 1-propanol concentration. The rate of appearance can be close to the rate of disappearance explaining the low values of kinetic orders (α_2 and α_3) obtained for propionaldehyde and acetaldehyde. At maximum light irradiance with a 400 ppm inlet concentration of

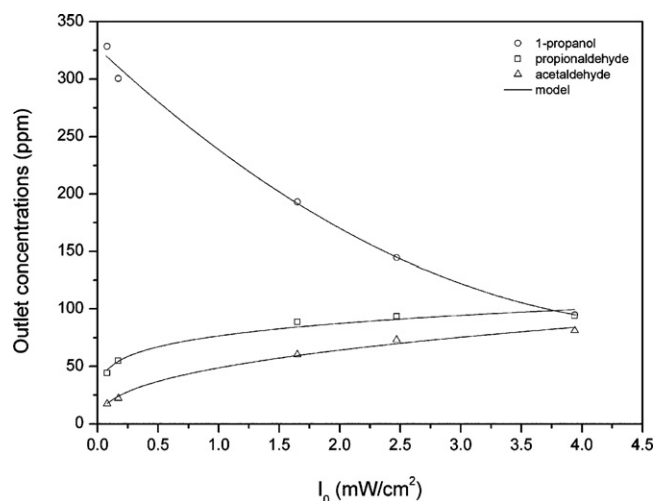


Fig. 9. Effect of the incident light irradiance on the 1-propanol and its by-product outlet concentrations after a 154 min illumination time. Regular conditions used were: total volume flow rate, $Q_v = 320 \text{ mL min}^{-1}$; relative humidity, $\text{RH} = 10\%$; photoreactor temperature, $T_R = 30^\circ\text{C}$; initial concentration, 1-propanol = 400 ppm; oxygen content, air (20 vol% O_2).

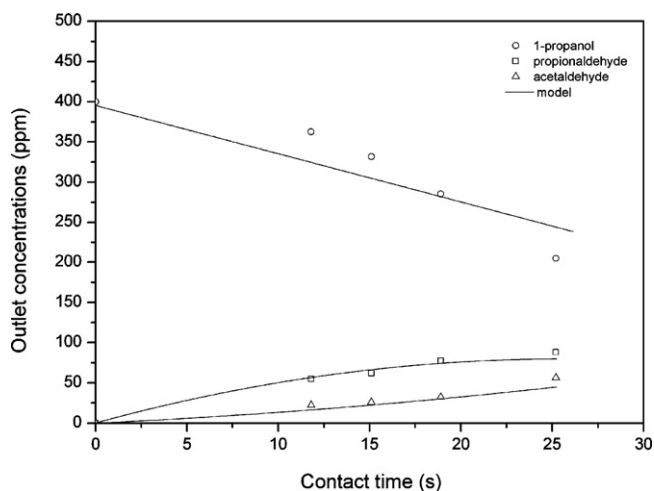


Fig. 10. Effect of the residence time on the 1-propanol and its by-product outlet concentrations after a 206 min illumination time. Regular conditions used were: incident light irradiance, $I_0 = 0.078 \text{ mW cm}^{-2}$; relative humidity, RH = 10%; photoreactor temperature, $T_R = 30^\circ\text{C}$; initial concentration, 1-propanol = 400 ppm; oxygen content, air (20 vol% O_2).

1-propanol, about 75% of 1-propanol is converted, 92 ppm of propionaldehyde and 84 ppm of acetaldehyde are produced in gas phase. The photocatalytic reactor seems to be inefficient, as it produces intermediates more toxic than the initial pollutant (1-propanol: $C_{\text{out}}/\text{TLV} = 0.5$; propionaldehyde: $C_{\text{out}}/\text{TLV} = 4.6$; acetaldehyde: $C_{\text{out}}/\text{TLV} = 0.8$). As previously indicated, the photoreactor efficiency could be improved with other experimental conditions such as a higher contact time. From Fig. 9, we can show that the outlet concentrations seem to be well fitted by the “two-site model”.

3.5. Effect of the contact time (gas flow)

The effect of contact time on 1-propanol, propionaldehyde and acetaldehyde outlet concentrations were investigated in the range of 25.2 s (150 mL min^{-1}) to 11.8 s (320 mL min^{-1}). From Fig. 10, we can observe that 1-propanol outlet concentration decreases from 400 to 200 ppm as the contact time is enhanced from 11.8 to 25.2 s. The propionaldehyde and acetaldehyde outlet concentrations seem to be well fitted by the previously established model. However, the predicted 1-propanol outlet concentration is not well fitted by the “two-site model”. This shape can be attributed to a possible competition of adsorption between 1-propanol and other by-products on the same adsorption site. Araña et al. [4,6] have mentioned the formation of propionaldehyde, propanoic acid and acetaldehyde during the 1-propanol photocatalytic degradation. Nimlos et al. have [9] investigated the photocatalytic degradation of ethanol and they have established the following reaction pathway: ethanol \rightarrow acetaldehyde \rightarrow acetic acid \rightarrow formaldehyde \rightarrow other products. Here we can consider that 1-propanol is degraded via the same sequence: 1-propanol \rightarrow propionaldehyde \rightarrow propanoic acid \rightarrow acetaldehyde \rightarrow other products. Several authors suggest that Type I site can accommodate only alcohols and acids and that Type II site can accommodate all of the organic compounds considered. In our case, we have only detected propionaldehyde and acetaldehyde in the gas phase. No qualitative and quantitative measurements are available on the propanoic acid formation in the gas phase. The absence of propanoic acid can be explained by its strong adsorption on the photocatalyst surface. Propanoic acid could be present in gas phase at very low concentrations and therefore not detectable by FID or GC/MS. An alteration to

photoreactor must be made in order to highlight the possible formation of propanoic acid at the TiO_2 surface.

3.6. Effect of the humidity content

Humidity content is well known to possess a key role in photocatalytic reactions. Consequently, it has been important to study the effect of humidity content on the 1-propanol conversion and on the selectivity of gaseous by-products. Selectivity (S) of propionaldehyde and acetaldehyde, which is based on carbon balance, is, respectively, defined as below:

$$S_{\text{propionaldehyde}} = \frac{[\text{propionaldehyde}]}{[\text{propanol}]_0 X}, \quad \text{CH}_3\text{CH}_2\text{CH}_2\text{OH} \rightarrow \text{CH}_3\text{CH}_2\text{CHO} \text{ (propionaldehyde)} \quad (21)$$

$$S_{\text{acetaldehyde}} = \frac{[\text{acetaldehyde}]}{\frac{3}{2}[\text{propanol}]_0 X}, \quad \text{CH}_3\text{CH}_2\text{CH}_2\text{OH} \rightarrow \frac{3}{2}\text{CH}_3\text{CHO} \text{ (acetaldehyde)} \quad (22)$$

where $[\text{propionaldehyde}]$ is the concentration of propionaldehyde produced, $[\text{propanol}]_0$ the inlet 1-propanol concentration, $[\text{acetaldehyde}]$ the concentration of acetaldehyde produced and X the 1-propanol conversion.

The effect of humidity content on the 1-propanol conversion and the by-product selectivity was investigated in the range of 0–30%. The experimental constraints used (volumetric flow rate in each way, thermostatic bath temperature, reactor temperature etc.) cannot deliver a relative humidity higher than 30%. From Fig. 11, it can be noticed that humidity content has a positive effect on 1-propanol conversion. Here we can see that 1-propanol conversion increases from 24 to 62% as the humidity content increases from 0 to 30%. Humidity content can improve the by-product abatement as the propionaldehyde and acetaldehyde selectivity decreases from 47 to 18% and from 10 to 3.6%, respectively. The hydroxyl radicals are known to be strong oxidants and they contribute to an increase in 1-propanol conversion in the presence of water vapour. The water molecules can be transformed into hydroxyl radicals (OH^\bullet) by reacting with the photogenerated holes (h^+) or superoxide radical ($\text{O}_2^{\bullet-}$)

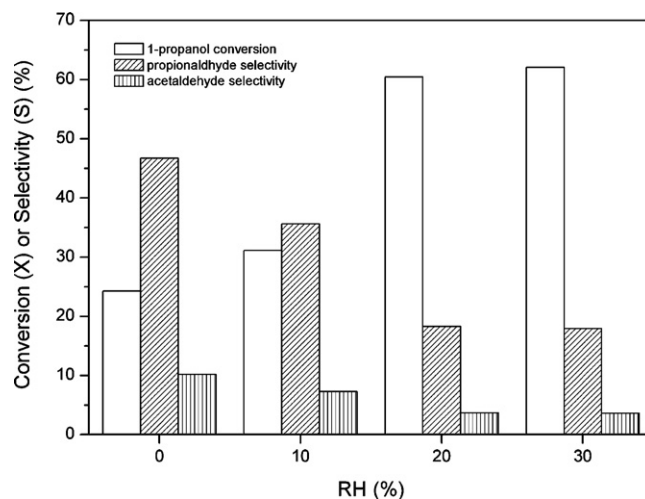
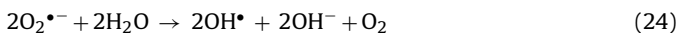


Fig. 11. Effect of water vapour on the 1-propanol conversion and the selectivity of its by-products after a 176 min illumination time. Regular conditions used were: total volume flow rate, $Q_v = 180 \text{ mL min}^{-1}$; incident light irradiance, $I_0 = 0.078 \text{ mW cm}^{-2}$; relative humidity, $T_R = 30^\circ\text{C}$; initial concentration, 1-propanol = 400 ppm; oxygen content, air (20 vol% O_2).

at the photocatalyst surface via the following reactions:

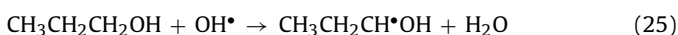


Benoît-Marquié et al. [8] and Pillai and Sahle-Demessie [13] have mentioned no significant effect of water vapour on alcohol photodegradation.

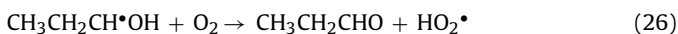
3.7. Mechanism of the photocatalytic degradation of 1-propanol

From Araña et al. [4,6], the photocatalytic degradation of aliphatic alcohols has been described by two different mechanisms which lead to the same result: (a) the combined attack of OH^\bullet radicals and oxygen and (b) the adsorbed alcoholates reaction with holes. In this present work, the mechanism (a) has been chosen. Several mechanisms on TiO_2 at the gas–solid interface are used to describe the photocatalytic degradation of alcohols. Here we have used the literature on mechanisms of homogeneous gas-phase reactions. The well-known homogeneous mechanisms have been used as a first approximation to explain the major by-products formation at the catalyst surface. Nimlos et al. [9] have used this approach to explain the products from the photocatalytic oxidation of chlorinated ethylenes.

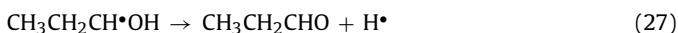
Nimlos et al. [9] have mentioned the possible formation of ethanol radical in aqueous-phase during the photocatalytic degradation of ethanol. This remark can be used to explain the possible formation of the 1-propanol radical. Adsorbed 1-propanol can react with a hydroxyl radical (OH^\bullet) to produce the 1-propanol radical as below [25]:



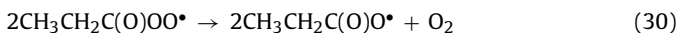
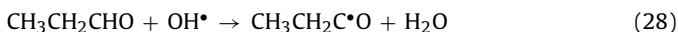
The 1-propanol radical can react with oxygen to form propionaldehyde via the following equation [26]:



The 1-propanol radical can be also decomposed by β scission with a cleavage of O–H bond in order to produce propionaldehyde and hydrogen radical:



In this present work, we have identified propionaldehyde as gaseous intermediate during the photocatalytic degradation of 1-propanol. Araña et al. [4,6] have also mentioned the formation of propionaldehyde during the photocatalytic degradation of this aliphatic alcohol. Then propionaldehyde can be directly oxidized by OH^\bullet to form a carbonyl radical [27] which can react with oxygen through the following series of reactions [28,29]:



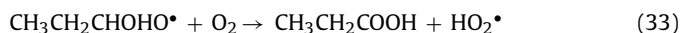
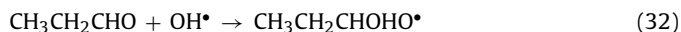
The carboxylate radical ($CH_3CH_2C(O)O^\bullet$) can be decomposed by β scission with a cleavage of C–C bond in order to produce an ethyl radical and carbon dioxide:



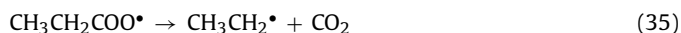
The formation of carbon dioxide has been highlighted by a homemade microreactor of methanation during the photocatalytic degradation of 1-propanol. However, for a reliable quantification of carbon dioxide, a chromatographic apparatus should be equipped with two distinct specific analytical columns and FIDs. In this present study, the detection of carbon dioxide was realised at 30 °C

with the same used-Porapak Q column for the quantification of 1-propanol. With this low oven temperature, 1-propanol is strongly adsorbed on the stationary phase of the analytical column involving a deterioration of the stationary phase and a quantitative determination of carbon dioxide.

Propionaldehyde can react with OH^\bullet to form propanoic acid through the following series of reactions:



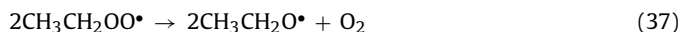
Here we have not observed propanoic acid in gas phase whereas Araña et al. [4,6] have mentioned its formation during the photocatalytic degradation of 1-propanol. The absence of propanoic acid can be explained by a strong adsorption on the photocatalyst surface. Nimlos et al. [9] and Benoît-Marquié et al. [8] have identified butanoic acid and acetic acid during the photocatalytic oxidation of 1-butanol and ethanol, respectively. It has been described that carboxylic acids are known to react by the photo-Kolbe mechanism with holes ($RCH_2COOH + h^+ \rightarrow RCH_2^\bullet + CO_2$). Propanoic acid can be directly oxidized by holes to form a propanoate radical. This radical is decomposed by β scission with a cleavage of C–C bond in order to produce the ethyl radical and carbon dioxide:



The ethyl radical can react with molecular oxygen to form the ethyl peroxy radical which can also be converted to the ethoxy radical by reactions with peroxy groups [30]:



Then the ethoxy radical can react with molecular oxygen to produce acetaldehyde and hydroperoxy radical via the following reactions [31,32]:



Araña et al. [4,6] have mentioned the formation of acetaldehyde during the photocatalytic degradation of 1-propanol. Several authors have detected esters which could be formed by the reactions of alcohols with carboxylic acids [9]. In this present work, no esters have been detected. It can be noted that the annular photoreactor is not equipped with a heating system allowing desorption of by-products adsorbed at the TiO_2 surface. The proposed mechanism seems to be adapted to explain the formation in gas phase of major by-products after photocatalytic oxidation of 1-propanol.

4. Conclusion

In this present work, we have adjusted the photodegradation rate to fit the destruction data for each compound, and we have used adsorption parameters determined previously (see Section 3.3) in order to predict the outlet concentrations. It has been demonstrated that the “*simple LH model*” was inadequate for fitting the 1-propanol conversion curve and that best fit could be obtained if intermediates were included. We have introduced the possibility of two adsorption sites: Type I site can accommodate only alcohols and acids and that Type II site accommodate all of the organic compounds considered.

The effect of initial concentration of pollutant was investigated and we found that the “*two-site model*” was adequate for fitting the 1-propanol, propionaldehyde and acetaldehyde curves. The effect of contact time on 1-propanol, propionaldehyde and acetaldehyde outlet concentrations was also investigated. It has been observed

that the 1-propanol outlet concentration is not well fitted by the “two-site model” only for Fig. 10. Nevertheless, the propionaldehyde and acetaldehyde outlet concentrations seem to be well fitted by the “two-site model”. A possible competition of adsorption 1-propanol and other by-products could take place on the same adsorption site. Several authors have reported the formation of carboxylic acids during the photocatalytic degradation of alcohols. A more complicated model, where propionic acid is taken into account, could be developed in order to obtain better results but no qualitative measurements are available on the propanoic acid formation in the gas phase because this specie is known to be very sticky and often at very low concentrations due to the high adsorption at the TiO₂ surface [9]. We have showed that humidity content increase enhanced the 1-propanol conversion and decreased the by-products selectivity.

Nevertheless, the proposed mechanism seems to be well adapted to explain the formation in gas phase of major by-products after photocatalytic degradation of 1-propanol. We have shown that the photocatalytic degradation of 1-propanol produced gaseous propionaldehyde and acetaldehyde which are more toxic than the initial pollutant. The photoreactor efficiency could be improved in order to reduce the by-product concentrations with other experimental conditions such as a higher contact time.

References

- [1] S. Shojania, R.D. Oleschuk, M.E. McComb, H.D. Gesser, A. Chow, The active and passive sampling of benzene, toluene, ethyl benzene and xylenes compounds using the inside needle capillary adsorption trap device, *Talanta* 50 (1999) 193–205.
- [2] J. Peral, D.F. Ollis, TiO₂ photocatalyst deactivation by gas-phase oxidation of heteroatom organics, *J. Mol. Catal. A Chem.* 115 (1997) 347–354.
- [3] A. Bouzaza, C. Vallet, A. Laplanche, Photocatalytic degradation of some VOCs in the gas phase using an annular flow reactor: determination of the contribution of mass transfer and chemical reaction steps in the photodegradation process, *J. Photochem. Photobiol. A Chem.* 177 (2006) 212–217.
- [4] J. Araña, J.M. Doña-Rodríguez, C.G.I. Cabo, O. González-Díaz, J.A. Herrera-Melián, J. Pérez-Peña, FTIR study of gas-phase alcohols photocatalytic degradation with TiO₂ and AC-TiO₂, *Appl. Catal. B Environ.* 53 (2004) 221–232.
- [5] J. Araña, J.M. Doña-Rodríguez, O. González-Díaz, E. Tello Rendón, J.A. Herrera Melián, G. Colón, J.A. Navío, J. Pérez Peña, Gas-phase ethanol photocatalytic degradation study with TiO₂ doped with Fe, Pd and Cu, *J. Mol. Catal. A Chem.* 215 (2004) 153–160.
- [6] J. Araña, J.M. Doña-Rodríguez, J.A.H. Melián, E.T. Rendón, O.G. Díaz, Role of Pd and Cu in gas-phase alcohols photocatalytic degradation with doped TiO₂, *J. Photochem. Photobiol. A Chem.* 174 (2005) 7–14.
- [7] J. Araña, J.M.D. Rodríguez, O.G. Díaz, J.A.H. Melián, J.P. Peña, Comparative study on the photocatalytic mineralization of homologous aliphatic acids and alcohols, *Appl. Surf. Sci.* 252 (2006) 8193–8202.
- [8] F. Benoît-Marquié, U. Wilkenhoner, V. Simon, A.M. Braun, E. Oliveros, M.-T. Maurette, VOC photodegradation at the gas-solid interface of a TiO₂ photocatalyst: Part I: 1-butanol and 1-butylamine, *J. Photochem. Photobiol. A Chem.* 132 (2000) 225–232.
- [9] M.R. Nimlos, E.J. Wolfrum, M.L. Brewer, J.A. Fennell, G. Bintner, Gas-phase heterogeneous photocatalytic oxidation of ethanol: pathways and kinetic modeling, *Environ. Sci. Technol.* 30 (1996) 3102–3110.
- [10] M.P. Paschoalino, J. Kiwi, W.F. Jardim, Gas-phase photocatalytic decontamination using polymer supported TiO₂, *Appl. Catal. B Environ.* 68 (2006) 68–73.
- [11] J. Peral, D.F. Ollis, Heterogeneous photocatalytic oxidation of gas-phase organics for air purification: acetone, 1-butanol, butyraldehyde, formaldehyde, and m-xylene oxidation, *J. Catal.* (2007) 554–565.
- [12] S. Pilkenton, S.J. Hwang, D. Raftery, Ethanol Photocatalysis on TiO₂-Coated optical microfiber, supported monolayer, and powdered catalysts: an in situ NMR study, *J. Phys. Chem. B* 103 (1999) 11152–11160.
- [13] U.R. Pillai, E. Sahle-Demessie, Selective oxidation of alcohols in gas phase using light-activated titanium dioxide, *J. Catal.* 211 (2002) 434–444.
- [14] E. Piera, J.A. Ayllon, X. Domenech, J. Peral, TiO₂ deactivation during gas-phase photocatalytic oxidation of ethanol, *Catal. Today* 76 (2002) 259–270.
- [15] J. Chen, D.F. Ollis, W.H. Rulkens, H. Bruning, Photocatalyzed oxidation of alcohols and organochlorides in the presence of native TiO₂ and metallized TiO₂ suspensions. Part (I). Photocatalytic activity and pH influence, *Water Res.* 33 (1999) 661–668.
- [16] N. Doucet, F. Bocquillon, O. Zahraa, M. Bouchy, Kinetics of photocatalytic VOCs abatement in a standardized reactor, *Chemosphere* 65 (2006) 1188–1196.
- [17] G. Vincent, A. Queffeuilou, P.M. Marquaire, O. Zahraa, Remediation of olfactory pollution by photocatalytic degradation process: study of methyl ethyl ketone (MEK), *J. Photochem. Photobiol. A Chem.* 191 (2007) 42–50.
- [18] C. Hachem, F. Bocquillon, O. Zahraa, M. Bouchy, Decolorization of textile industry wastewater by the photocatalytic degradation process, *Dyes Pigments* 49 (2001) 117.
- [19] J. Villermaux, Génie de la réaction chimique: conception et fonctionnements des réacteurs, Lavoisier, Paris, 1993.
- [20] O. Carp, C.L. Huisman, A. Reller, Photoinduced reactivity of titanium dioxide, *Prog. Solid State Chem.* 32 (2004) 33.
- [21] M. Lewandowski, D.F. Ollis, A Two-site kinetic model simulating apparent deactivation during photocatalytic oxidation of aromatics on titanium dioxide (TiO₂), *Appl. Catal. B Environ.* 43 (2003) 309–327.
- [22] K.-H. Wang, H.-H. Tsai, Y.-H. Hsieh, The kinetics of photocatalytic degradation of trichloroethylene in gas phase over TiO₂ supported on glass bead, *Appl. Catal. B Environ.* 17 (1998) 313–320.
- [23] D.F. Ollis, E. Pelizzetti, N. Serpone, Photocatalyzed destruction of water contaminants, *Environ. Sci. Technol.* 25 (1991) 1522–1529.
- [24] G. Vincent, P.M. Marquaire, O. Zahraa, Abatement of volatile organic compounds using an annular photocatalytic reactor: study of gaseous acetone, *J. Photochem. Photobiol. A Chem.* 197 (2008) 177–189.
- [25] A. Hatipoglu, Z. Cinar, A QSAR study on the kinetics of the reactions of aliphatic alcohols with the photogenerated hydroxyl radicals, *J. Mol. Struct. THEOCHEM* 631 (2003) 189–207.
- [26] A. Miyoshi, H. Matsui, N. Washida, Rates of reaction of hydroxyalkyl radicals with molecular oxygen, *J. Phys. Chem.* 94 (1990) 3016–3019.
- [27] J.A. Kerr, D.W. Stocker, The kinetics and mechanism of the photo-oxidation of propionaldehyde under simulated atmospheric conditions, *J. Photochem.* 28 (1985) 475–489.
- [28] R.R. Baldwin, R.W. Walker, D.H. Langford, Oxidation of propionaldehyde in aged boric-acid-coated vessels. Part 2. Analytical results, *Trans. Faraday Soc.* 65 (1969) 806–815.
- [29] C.A. McDowell, L.K. Sharples, The photochemical oxidation of aldehydes in the gaseous phase. Part III. The absolute values of the velocity constants for the velocity constants for the propagating and terminating steps in the photochemical oxidation of acetaldehyde and propionaldehyde, *Can. J. Chem.* 36 (1958) 268–278.
- [30] C.Y. Sheng, J.W. Bozzelli, A.M. Dean, A.Y. Chang, Detailed kinetics and thermochemistry of C₂H₅ + O₂: reaction kinetics of the chemically activated and stabilized CH₃CH₂OO* adduct, *J. Phys. Chem. A* 106 (2002) 7276–7293.
- [31] R. Atkinson, D.L. Baulch, R.A. Cox, R.F. Hampson Jr., J.A. Kerr, J. Troe, Evaluated kinetic and photochemical data for atmospheric chemistry: supplement IV. IUPAC subcommittee on gas kinetic data evaluation for atmospheric chemistry, *J. Phys. Chem. Ref. Data* 21 (1992) 1125–1568.
- [32] D. Bauer, J.N. Crowley, G.K. Moortgat, The UV absorption spectrum of the ethylperoxy radical and its self-reaction kinetics between 218 and 333 K, *J. Photochem. Photobiol. A Chem.* 65 (1992) 329–344.